Jurnal Penelitian Fisika dan Aplikasinya (JPFA) *Volume 8, Issue 1, June 2018*
p-ISSN: 2087-9946 DOI: 10.26740/jpfa.v8n1.p1-9
e-ISSN: 2477-1775 http://journal.unesa.ac.id/index.php/jpfa

Research Article

Combination of Coprecipitation and Sonochemical Methods in Synthesizing Spinel Hausmannite Nanomaterial

Nurul Hidayat [a], Ahmad Taufiq [b], Sunaryono [c], Samsul Hidayat [d], Heriyanto [e], and Era Budi Prayekti [f]

Department of Physics, Faculty of Mathematics and Natural Sciences, Universitas Negeri Malang
Jl. Semarang 5, Malang 65145, Indonesia

e-mail: [a] nurul.hidayat.fmipa@um.ac.id, [b] ahmad.taufiq.fmipa@um.ac.id, [c] sunaryono.fmipa@um.ac.id, [d] samsul.hidayat.fmipa@um.ac.id, [e] heriyanto.fmipa@um.ac.id, and [f] era.budi.fmipa@um.ac.id

Abstract

As it has been widely known that the spectacular characteristics of nanomaterials are strongly dependent on their particle size, crystal structure, and molecular arrangement. The fine structure formation of nanomaterials is inevitable in an attempt of optimizing their promising applications in various fields. One of the notable nanomaterials up to now is hausmannite or Mn_3O_4. This paper presents a combination of coprecipitation and sonochemical routes in a concurrent way to produce spinel-structured hausmannite nanomaterials. The pH was varied during the synthesis at values of 9, 10, 11, 11.5, and 12. The crystal structure properties were evaluated by X-ray diffractometry (XRD) with the diffraction angle range of 15° - 80°. The functional groups were investigated by Fourier transform infrared (FTIR) spectrometry having wavenumber from 400 to 4000 cm^{-1}. In this study, pH 10 was found to be the best synthesis parameter in producing Mn_3O_4. Both XRD and FTIR data analyses have agreed on the formation of spinel hausmannite nanomaterials.

Keywords: *coprecipitation-sonochemistry, Mn_3O_4 nanomaterial, crystal structure, molecular structure*

Kombinasi Metode Kopresipitasi dan Sonokimia dalam Sintesis Nanomaterial Spinel Hausmanit

Abstrak

Sebagaimana telah diketahui secara luas bahwa karakteristik spektakuler dari nanomaterial sangat bergantung pada ukuran partikel, struktur kristal dan tatanan molekulernya. Pembentukan fine structure dari nanomaterial menjadi sebuah keharusan dalam upaya memaksimalkan potensi aplikasinya di berbagai bidang. Salah satu nanomaterial yang hingga detik ini menjadi primadona adalah hausmanit atau Mn_3O_4. Penelitian ini memaparkan penggabungan metode kopresipitasi dan sonokimia secara bersamaan untuk menghasilkan nanomaterial hausmanit berstruktur spinel. pH selama proses sintesis divariasi pada nilai 9, 10, 11, 11,5 dan 12. Karakteristik struktur kristal diuji dengan instrumen X-ray diffraction (XRD) dengan rentang sudut difraksi 15°-80°. Gugus fungsi diuji dengan menggunakan spektrometer Fourier transform infrared (FTIR) dengan rentang bilangan gelombang dari 400 hingga 4000 cm^{-1}. Pada penelitian ini, nilai pH 10 merupakan parameter sintesis terbaik untuk memproduksi Mn_3O_4. Kedua analisis data (XRD dan FTIR) menunjukkan pembentukan dari nanomaterial spinel hausmannite.

Kata Kunci: *kopresipitasi-sonokimia, nanomaterial Mn_3O_4, struktur kristal, struktur molekuler.*

PACS: 61.50.-f, 73.63.Bd, 78.67.Bf

Article History: Received: October 26, 2017 Decided to resubmit (Round 1): November 12, 2017
Revised (Round 1): December 24, 2017 Approved with minor revision: February 17, 2018
Accepted: February 27, 2018 Published: June 30, 2018

How to cite: Hidayat N, Taufiq A, Sunaryono, Hidayat S, Heriyanto, and Prayekti EB. Combination of Coprecipitation and Sonochemical Methods in Synthesizing Spinel Hausmannite Nanomaterial. *Jurnal Penelitian Fisika dan Aplikasinya (JPFA)*. 2018; **8**(1): 1-9. DOI: https://doi.org/10.26740/jpfa.v8n1.p1-9.

I. INTRODUCTION

Research of nanomaterial and nanotechnology has become a trend for the last decades. In the past two years for example, transition metal oxides are reported as promising nanomaterials in many applications especially as gas sensor and electrochemical agents [1–3]. Even Mn_3O_4 is projected as super-sensitive electrochemical detector for hydrogen peroxide [4], photocatalyst [5], electroactive electrode of supercapacitor [6], and detector of nimorazole to heal head and neck cancers [7]. Therefore, the preparation of highly homogeneous Mn_3O_4 nanomaterial should be continually optimized.

Hausmannite, a mineral with chemical formula of Mn_3O_4, crystallizes with a normal spinel structure [8]. Mn_3O_4 undergoes tetragonal distortion to the *c* axis and based on the inorganic crystal structure database (ICSD) with the collection code of 76088, Mn_3O_4 has lattice parameters of $a = b = 5.765$ Å and $c = 9.442$ Å in the space group of 141/AMDS. The divalent manganese ions are on the tetrahedral site and the trivalent manganese ions are on the octahedral site of the normal spinel structure [8], as visualized in Figure 1.

To date, Mn_3O_4 nanoparticles have been successfully produced using simple coprecipitation approach at low temperature of 70 °C [9]. This method is claimed to be more reliable from other methods, like spray pyrolysis approach [10] which requires relaitively high temperature of 750 °C. Meanwhile, sonochemical method is also believed as one of the alternatives to obtain nanometer-sized material with high surface area characteristic [11-13]. This method, by the use of ultrasonic wave to trigger the activation of chemical reaction through acoustic cavitation mechanism [14], has been successfully applied to obtain Mn_3O_4 nanomaterial [15].

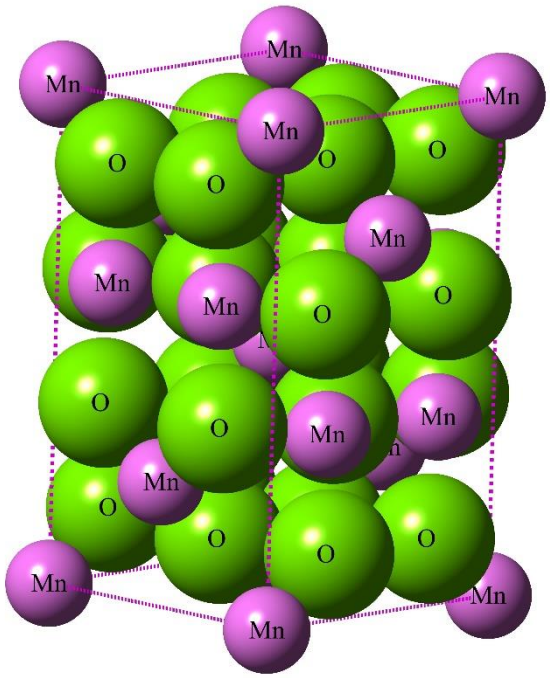

Figure 1. 3D Crystal Structure Model of Mn_3O_4

In coprecipitation method, salts such as $FeCl_2$ and $MnCl_2 \cdot 4H_2O$ [16] are involved as the basic materials prior to mixing with acid-based solvents [9]. The prepared solution is wisely stirred while adding precipitating agent to produce homogenous nanomaterial.

The effective precipitating agent is NH_4OH because the residu can be removed easily by heating [16]. On another side, acoustic cavitation in sonochemical process is the manifestation of the desolation of acoustic, forming, and the growth as well as the collapse of the small bubble within the liquid bombarded by ultrasonic energy [12]. The bubble stability stimulates local heating in the cold liquid to produce nanomaterials [17].

Based on the previous work, the combination of coprecipitation and sonochemical methods were employed to fabricate nanoparticles with excellent properties especially in terms of phase purity and crystal size [18]. However, the variation of pH in both Mn_3O_4-synthesis processes has not yet been reported. Therefore, in this present paper, the variation of pH is our primary research focus.

II. RESEARCH METHOD

Coprecipitation process was executed by dropping NH_4OH (PA) into $MnCl_2{\cdot}4H_2O$ (PA) solution for 30 minutes on a magnetic stirrer at room temperature. The volume of NH_4OH was varied to control the pH value in the range of 9 to 12. The solution was then sonicated for 30 minutes with frequency of 40 kHz. The result of sonication was rinsed and filtered to obtain normal pH. The Mn_3O_4 nanomaterial powder was obtained after drying process at temperature of 100 °C for 60 minutes.

The produced Mn_3O_4 nanoparticles were characterized by means of XRD with diffraction angle range of 15° - 80° to investigate the crystal phase, crystal structure, and crystal size. The phase identification and its quantification were analyzed using relative intensity ratio (RIR) and Rietveld methods, respectively. Functional groups of chemical bond in the samples were also verified through Fourier transform infrared (FTIR) spectroscopy.

III. RESULTS AND DISCUSSION

The XRD data of Mn_3O_4 sample synthesized using the combination of coprecipitation and sonochemical methods in various pH values are presented in Figure 2. Clearly, XRD data of all samples have similar profiles.

The search-match analysis reveals that all samples contain mainly Mn_3O_4 phase that crystallizes with tetragonal normal spinel structure with space group of I41/AMDS and PDF (powder difraction file) reference code of 01-080-0382. All diffraction peaks, indicating the hausmannite-Mn_3O_4, are labelled by the following Bragg planes: (101), (112), (200), (103), (211), (004), (220), (204), (015), (312), (303), (321), (224), (400), (305), (413), (404), and (325). The data analysis shows that the only sample with the best homogeneity of Mn_3O_4 phase goes to sample with pH = 10. The other four samples have an additional small diffraction peak at 26° indicating the presence of a minor phase. This minor phase is manganite ($HMnO_2$) with PDF reference code number of 01-088-0649. However, the content of $HMnO_2$ in the samples is relatively small.

The RIR method for the need of semi-quantitative analysis uncoveres that the manganite within the samples is less than 10%. In detail, the percentage of manganite detected in the samples with pH parameters of 9, 11, 11.5, and 12, are 8%, 4%, 5%, and 9%, respectively. Hence, pH 10 is the best parameter to prepare the hausmannite-Mn_3O_4 with combined coprecipitation and sonochemical methods.

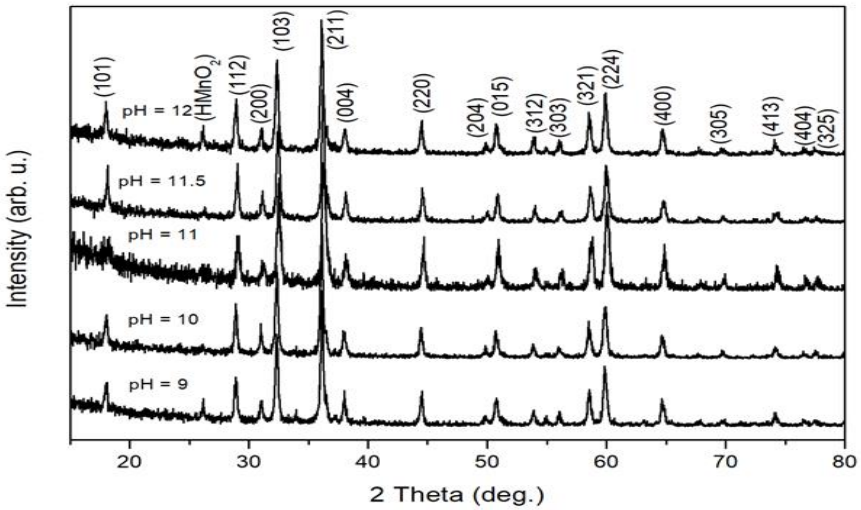

Figure 2. XRD Patterns of Mn_3O_4 Nanomaterials Produced by Coprecipitation-Sonochemical Approach

One of the ways to emit manganite is heating the sample at the temperature of 300 °C since manganite will be decomposed at the temperature of 250 °C [19]. The low intensity of diffraction and the width of the peak indicate qualitatively that the size of Mn_3O_4 crystal has been in nanometer order.

The characteristics of the crystallographical parameter of the produced spinel hausmannite were analyzed using Rietveld method with Rietica software [20]. The profile of Voight (How. Asym) in Rietica could track the mean of Scherrer method-based crystal size. The example of output plot of analysis results are presented in Figure 3. The results of refinement are very good due to the good fit between the measured and calculated diffraction profiles. Good of fitness (GoF), as the parameter of the suitability of the analysis results of Rietveld refinement, has been in the acceptable number (under 4%) [20]. The GoF values of Rietveld analysis result and all XRD data in this research are in the range of 0.5 - 1%. Therefore, these analysis results can be used for the valid information of crystal structure and crystal size.

Table 1. Crystallographical Parameters of Mn_3O_4 Nanomaterials Prepared from Coprecipitation-Sonochemical Method

Sample of Mn_3O_4	Lattice parameter (Å)		Crystal size (nm)
	$a = b$	c	
pH = 9	5.7644(6)	9.4741(12)	55.25(12)
pH = 10	5.7634(9)	9.4669(20)	57.07(20)
pH = 11.5	5.7636(6)	9.4663(20)	51.80(10)
pH = 11	5.7680(6)	9.4763(20)	63.10(30)
pH = 12	5.7642(9)	9.4652(14)	56.22(15)

As a note, the number in the bracket presented in Table 1 is the standard deviation. 5.7644(6) Å means (5.7644 ± 0.0006) Å and 55.25(12) nm means (55.25 ± 0.12) nm, and so forth. Referring to Table 1, the crystal structure of Mn_3O_4 in the sample is tetragonal normal spinel with a lattice parameters of $a = b \neq c$ and $\alpha = \beta = \gamma = 90°$.

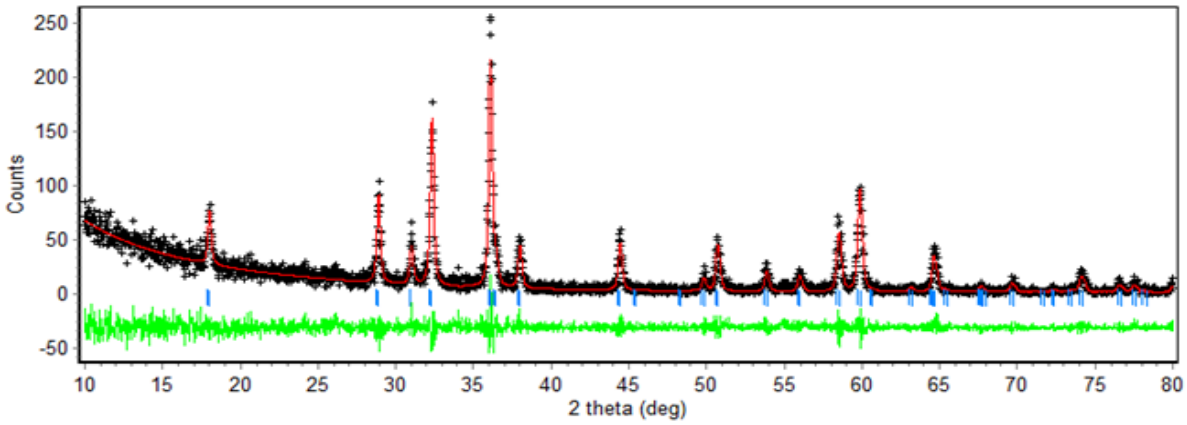

Figure 3. Output Plot of Rietveld Analysis Using Rietica for the Mn_3O_4 Nanomaterial at pH = 10.
The calculated data and the measured data are respectively represented by the solid line and by the plus sign (+). The green line at the bottom is the difference between the measured and calculated data.

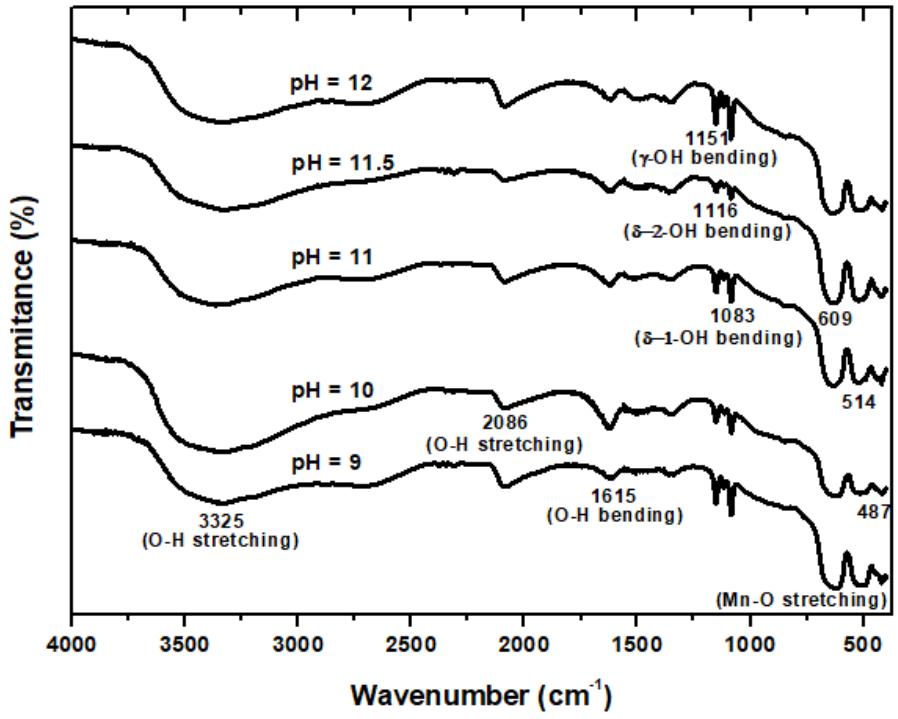

Figure 4. FTIR Spectra of Mn_3O_4 Nanomaterials Prepared by Coprecipitation-Sonochemical Method

Analysis of crystallite size is very significant since it is one of the principal characteristics of nanomaterials. Although electron microscopes are sophisticated to "see" accurately the nanometric dimension of materials, XRD can be an alternative to characterize crystallite size of nanomaterials. The widening of XRD peak can be used as a fingerprint of nanometer- sized particles since the crystal size of XRD data analysis with Rietveld method is claimed to be close to the results of electron microscopes [21]. The analysis results of crystallite size as presented in Table 1 shows that the crystallite size of all samples is less than 100 nm; this means that the samples of synthesis results are categorized as nanomaterials. The crystallite size obtained in this research is slightly smaller compared to the crystal size of Mn_3O_4 prepared using coprecipitation method [9].

Our present study exposes that the combination of coprecipitation and sonochemical methods enables the use of room temperature during stirring the raw materials with NH_4OH to result in nano-sized Mn_3O_4. It is a benefit compared to coprecipitation method that needs the temperature of 70 °C to form Mn_3O_4 nanomaterials [9]. On the other side, the reported sonochemical method has resulted in Mn_3O_4 nanomaterials [22] but with higher temperature, i.e. 50 °C, for one hour. Even compared to the same Mn_3O_4-synthesis route as reported in reference [18], our research was relatively faster in terms of the synthesis duration and lower in terms of temperature required in the coprecipitation and ultrasonication precesses.

The forming of spinel hausmannite nanomaterial is the manifestation of coprecipitation and sonochemical processes. Meanwhile, the chemical reaction during the coprecipitation process is given in Eq. (1) [23] and during the sonochemical process (after modifying precursor) is given in Eq. 2 [14].

$$3MnCl_2{\cdot}4H_2O + 6NH_4OH \rightarrow Mn_3O_4 + 6NH_4Cl + 14H_2O + H_2 \quad (1)$$

Taking into consideration Eq. (1), the manganese ions were reduced in NH_4OH media so that they decompose into MnO and then oxidise become Mn_3O_4 [24]. The use of ultrasonic irradiation during the precipitation process may decrease the duration of precipitation and ensure the homogeneity of Mn^{3+} cation distributions in the spinel crystal of Mn_3O_4 [22].

Additionally, based on the lattice parameters provided in Table 1, the spinel structure of Mn_3O_4 undergoes tetragonal distortion. This distortion is the physical implication of the active Jahn-Teller effect as the basis of the instability of the trivalent manganese ions (d^4) when they occupy octahedral sites and form a close-packed arrangement. Meanwhile, the divalent manganese (d^{10}) ions tend to occupy tetrahedral sites [25].

From crystal field viewpoint, the extension in lattice parameter *c* was initiated by the extension of *z*-axis in the octahedral complexes [26]. In other words, the octahedral complexes with central trivalent manganese ions has electron configuration of $t_{2g}^3\ e_g^1$ at the weak field, not $t_{2g}^4\ e_g^0$ that stimulates the appearance of the strong field [26].

The FTIR data of all samples are presented in Figure 3. Noticeably, there is a relatively large absorption at infrared wavenumbers of 3325 cm^{-1} and 2086 cm^{-1} identified as O-H strain and 1615 cm^{-1} as the absorption of water molecule on the hausmannite [27-28]. This absorption of water molecule informs that hausmannite as the synthesis result (with a few weight fraction of manganite) has a characteristic of high surface area as the indication of nanomaterial formation. The infrared absorption at 487 cm^{-1} and 609 cm^{-1} associates with Mn-O strain mode on the octahedral and tetrahedral sites [28]. These findings clarify the formation of normal spinel structure of Mn_3O_4. A strain mode of Mn-O also appears at 514 cm^{-1} [19]. The three consecutive absorption peaks at 1151 cm^{-1}, 1116 cm^{-1}, and 1083 cm^{-1}, indicates respectively O-H bending in the form of γ-OH, δ-2-OH, and δ-1-OH [29].

IV. CONCLUSION

The coprecipitation and sonochemical methods with five variations of pH have been successfully combined in the preparation of Mn_3O_4 hausmannite nanomaterials with crystallite size of about 55 nm. The results of phase identification of XRD data shows that the hausmannite tetragonal spinel crystal has been well formed although there is a small amount of manganite as the impurity.

Furthermore, according to the analysis results of Rietveld method-based XRD, pH 10 is the most optimum synthesis parameter for it contains hausmannite with the highest phase purity. On another side, FTIR data reveals that there are Mn-O strecthing on the octahedral and tetrahedral sites that confirm the formation of normal hausmannite Mn_3O_4 spinel structure.

ACKNOWLEDGMENT

The authors would like to deliver the greatest gratitude to Faculty of Mathematics and Natural Sciences, Universitas Negeri Malang (State University of Malang) that has provided a research grant with the Number of Assignment Letter of 6.6.12/UN32.3/PP/2016

REFERENCES

[1] Wang MY, Shen T, Wang M, Zhang DE, Tong Z, and Chen J. One-pot Synthesis of α-Fe_2O_3 Nanoparticles-Decorated Reduced Graphene Oxide for Efficient Nonenzymatic H_2O_2 Biosensor. *Sensors and Actuators B: Chemical*. 2014; **190**: 645–650. DOI: https://doi.org/10.1016/j.snb.2013.08.091.

[2] Zhang Y, Xie J, Xiao S, Yang Z, Pang P, Bai W, and Gao Y. Facile and Controllable Synthesis of Prussian Blue Nanocubes on TiO_2–graphene Composite Nanosheets for Nonenzymatic Detection of Hydrogen Peroxide. *Analytical Methods*. 2014; **6**(24): 9761–9768. DOI: https://doi.org/10.1039/C4AY02418D.

[3] Lin TS and Lee CT. Homostructured ZnO-based Metal-Oxide-Semiconductor Field-Effect Transistors Deposited at Low Temperature by Vapor Cooling Condensation System. *Applied Surface Science*. 2015; **354**(Part A): 71–73. DOI: https://doi.org/10.1016/j.apsusc.2014.12.179.

[4] Zeng F, Pan Y, Yang Y, Li Q, Li G, Hou Z, and Gu G. Facile Construction of Mn_3O_4-MnO_2 Hetero-Nanorods/Graphene Nanocomposite for Highly Sensitive Electrochemical Detection of Hydrogen Peroxide. *Electrochimica Acta*. 2016; **196**: 587–596. DOI: https://doi.org/10.1016/j.electacta.2016.03.031.

[5] Sheikhshoaie I, Ramezanpoura S, and Khatamian M. Synthesis and Characterization of Thallium Doped Mn_3O_4 as Superior Sunlight Photocatalysts. *Journal of Molecular Liquids*. 2017; **238**: 248-253. DOI: https://doi.org/10.1016/j.molliq.2017.04.088.

[6] Bui PTM, Song JH, Li ZY, Akhtar MS, and Yang OB. Low Temperature Solution Processed Mn_3O_4 Nanoparticles: Enhanced Performance of Electrochemical Supercapacitors. *Journal of Alloys and Compounds*. 2017; **694**: 560-567. DOI: https://doi.org/10.1016/j.jallcom.2016.10.007.

[7] Umamaheswari R, Akilarasan M, Chen SM, Cheng YH, Mani V, Kogularasu S, Al-Hemaid FMA, Ali MA, and Liu X. One-pot Synthesis of Three-Dimensional Mn_3O_4 Microcubes for High-Level Sensitive Detection of Head and Neck Cancer Drug Nimorazole. *Journal of Colloid and Interface Science*. 2017; **505**: 1193-1201. DOI: https://doi.org/10.1016/j.jcis.2017.07.006.

[8] Kaczmarczyk J, Zasada F, Janas J, Indyka P, Piskorz W, Kotarba A, and Sojka Z. Thermodynamic Stability, Redox Properties, and Reactivity of Mn_3O_4, Fe_3O_4, and Co_3O_4 Model Catalysts for N_2O Decomposition: Resolving the Origins of Steady Turnover. *ACS Catalysis*. 2016; **6**(2): 1235–1246. DOI: https://doi.org/10.1021/acscatal.5b02642.

[9] Taufiq A, Triwikantoro, Pratapa S, and Darminto. Sintesis Partikel Nano $Fe_{3-x}Mn_xO_4$ Berbasis Pasir Besi dan Karakterisasi Struktur serta Kemagnetannya. *Jurnal*

Nanosains & Nanoteknologi. 2008; **1**(2): 68–73.

[10] Konstantinov K, Ng SH, Wang JZ, Wang GX, Wexler D, and Liu HK. Nanostructured PbO Materials Obtained in situ by Spray Solution Technique for Li-Ion Batteries. *Journal of Power Sources*. 2006; **159**(1): 241–244. DOI: https://doi.org/10.1016/j.jpowsour.2006.04.029.

[11] Troia A, Pavese M, and Geobaldo F. Sonochemical Preparation of High Surface Area $MgAl_2O_4$ Spinel. *Ultrasonics Sonochemistry*. 2009; **16**(1): 136–140. DOI: https://doi.org/10.1016/j.ultsonch.2008.06.001.

[12] Ohayon E and Gedanken A. The Application of Ultrasound Radiation to the Synthesis of Nanocrystalline Metal Oxide in a Non-Aqueous Solvent. *Ultrasonics Sonochemistry*. 2010; **17**(1): 173–178. DOI: https://doi.org/10.1016/j.ultsonch.2009.05.015.

[13] Hidayat N, Taufiq A, Diantoro M, Nasikhudin, Fuad A, and Hidayat A. Aplikasi Kavitasi Akustik untuk Sintesis Nanomaterial Hetaerolite ($ZnMn_2O_4$) serta Karakteristik Geometri Kristalnya. *Proceeding of Seminar Nasional MIPA*, Universitas Negeri Malang. 2010.

[14] Xu H, Zeiger BW, and Suslick KS. Sonochemical Synthesis of Nanomaterials. *Chemical Society Reviews*. 2013; **42**(7): 2555–2567. DOI: https://doi.org/10.1039/C2CS35282F.

[15] Askarinejad A and Morsali A. Direct Ultrasonic-Assisted Synthesis of Sphere-like Nanocrystals of Spinel Co_3O_4 and Mn_3O_4. *Ultrasonics Sonochemistry*. 2009; **16**(1): 124–131. DOI: https://doi.org/10.1016/j.ultsonch.2008.05.015.

[16] Bahtiar S, Taufiq A, Sunaryono, Hidayat A, Hidayat N, Diantoro M, Mufti N, and Mujamilah. Synthesis, Investigation on Structural and Magnetic Behaviors of Spinel M-Ferrite [M = Fe; Zn; Mn] Nanoparticles from Iron Sand. *IOP Conference Series: Materials Science and Engineering*. 2017; **202**: 012052. DOI: https://doi.org/10.1088/1757-899X/202/1/012052.

[17] Suslick KS, Didenko Y, Fang MM, Hyeon T, Kolbeck KJ, McNamara III WB , Mdleleni MM, and Wong MM. Acoustic Cavitation and Its Chemical Consequences. *Philosophical Transactions of the Royal Society A: Mathematical, Physical and Engineering Sciences*. 1999; **357**(1751): 335–353. DOI: https://doi.org/10.1098/rsta.1999.0330.

[18] Tholkappiyan R, Naveen AN, Vishista K, and Hamed F. Investigation on Electrochemical Performance of Hausmannite Mn_3O_4 Nanoparticles by Ultrasonic Irradiation Assisted Co-precipitation Method for Supercapacitor Electrodes. *Journal of Taibah University for Science*. 2017; Article in press. DOI: https://doi.org/10.1016/j.jtusci.2017.07.001.

[19] Li F, Wu J, Qin Q, Li, and Huang X. Facile Synthesis of γ-MnOOH Micro/nanorods and Their Conversion to β-MnO_2, Mn_3O_4. *Journal of Alloys and Compounds*. 2010; **492**(1–2): 339–346. DOI: https://doi.org/10.1016/j.jallcom.2009.11.089.

[20] Hill RJ and Howard CJ. *A Computer Program for Rietveld Analysis of Fixed Wavelength X-ray and Neutron Powder Diffraction Patterns*. Australian Atomic Energy Commission, Research Establishment, Lucas Heights Research Laboratories; 1986.

[21] Pratapa S, Susanti L, Insany YAS, Alfiati Z, Hartono B, Mashuri, Taufiq A, Fuad A, Triwikantoro, Baqiya MA, Purwaningsih S, Yahya E, and Darminto. XRD Line-broadening Characteristics of M-oxides (M = Mg, Mg-Al, Y, Fe) Nanoparticles Produced by Coprecipitation Method. *AIP Conference Proceedings*. 2010; **1284**(1): 125-128. DOI: https://doi.org/10.1063/1.3515533.

[22] Baykala A, Kavas H, Durmuşa Z, Demira M, Kazanc S, Topkayac R, and Toprak MS. Sonochemical synthesis and Characterization of Mn_3O_4 Nanoparticles. *Central European Journal of Chemistry*. 2010; **8**(3): 633–638. DOI: https://doi.org/10.2478/s11532-010-0037-8.

[23] Taufiq A, Sunaryono, Putra EGR, Okazawa A, Watanabe I, Kojima N, Pratapa S, and Darminto. Nanoscale Clustering and Magnetic Properties of $Mn_xFe_{3-x}O_4$ Particles Prepared from Natural Magnetite. *Journal of Superconductivity and Novel Magnetism*. 2015; **28**(9): 2855–2863. DOI: https://doi.org/10.1007/s10948-015-3111-9.

[24] Dhaouadi H, Ghodbane O, Hosni F, and Touati F. Mn_3O_4 Nanoparticles: Synthesis, Characterization, and Dielectric Properties. *ISRN Spectroscopy*. 2012; **2012**: 894385. DOI: https://doi.org/10.5402/2012/894385.

[25] Menaka, Qamar M, Lofland SE, Ramanujachary KV, and Ganguli AK. Magnetic and Photocatalytic Properties of Nanocrystalline $ZnMn_2O_4$. *Bulletin of Materials Science*. 2009; **32**(3): 231–237. https://doi.org/10.1007/s12034-009-0035-7.

[26] Effendi E. *Perspektif Baru Kimia Koordinasi Jilid 1*. Malang: Bayumedia Publishing; 2007.

[27] Baykal A, Köseoğlu Y, and Şenel M. Low Temperature Synthesis and Characterization of Mn_3O_4 Nanoparticles. *Central European Journal of Chemistry*. 2007; **5**(1): 169–176. DOI: https://doi.org/10.2478/s11532-006-0064-7.

[28] Rui S, Hong-Jun W, and Shou-Hua F. Solvothermal Preparation of Mn_3O_4 Nanoparticles and Effect of Temperature on Particle Size. *Chemical Research in Chinese Universities*. 2012; **28**(4): 577–580. Available from: http://www.cjcu.jlu.edu.cn/hxyj/EN/abstract/abstract15584.shtml.

[29] Li Z, Bao H, Miao X, and Chen X. A Facile Route to Growth of γ-MnOOH Nanorods and Electrochemical Capacitance Properties. *Journal of Colloid and Interface Science*. 2011; **357**(2): 286–291. DOI: https://doi.org/10.1016/j.jcis.2011.02.011.